JOURNAL OF SPACECRAFT AND ROCKETS
Vol. 43, No. 4, July–August 2006

Engineering Notes

ENGINEERING NOTES are short manuscripts describing new developments or important results of a preliminary nature. These Notes should not exceed 2500 words (where a figure or table counts as 200 words). Following informal review by the Editors, they may be published within a few months of the date of receipt. Style requirements are the same as for regular contributions (see inside back cover).

Modeling and Simulation of Turbulent Reacting Flow Around a Hypersonic Space Probe

N. T.-H. Nguyen-Bui* and G. Duffa†
Commissariat à l'Énergie Atomique, 33114 Le Barp, France

Nomenclature

A	=	preexponential factor, (m^3, mole, s, K)
C	=	mass fraction
C_p	=	specific heat at constant pressure, $J \cdot kg^{-1} \cdot K^{-1}$
H	=	total enthalpy, $J \cdot m^{-3}$
h_α	=	enthalpy of αth species, $J \cdot m^{-3}$
K_f, K_b	=	reaction-rate coefficients, (m^3, mole, s)
k	=	turbulent kinetic energy, $J \cdot m^{-3}$
$\mathcal{M}$	=	molar mass, $kg \cdot mol^{-1}$
n	=	exponential factor
ne	=	number of species
nr	=	number of gaseous reactions
P	=	total pressure, Pa
$\mathcal{P}$	=	probability density function
Pr_t	=	turbulent Prandtl number, $\mu_t C_p/\lambda_t$
Re_t	=	turbulent Reynolds number, $\rho k/\omega\mu$
T	=	temperature, K
T_A	=	activation temperature, K
t	=	time, s
U	=	velocity, $m \cdot s^{-1}$
x	=	space, m
λ	=	thermal conductivity, $W \cdot m^{-1} \cdot K^{-1}$
μ	=	viscosity, $kg \cdot m^{-1} \cdot s^{-1}$
ν', ν''	=	forward and backward stochiometric coefficients
ρ	=	density, $kg \cdot m^{-3}$
σ_C	=	mass fraction variance
$\bar{\bar{\sigma}}$	=	stress tensor, $kg \cdot m^{-1} \cdot s^{-2}$
τ	=	turbulent integral time scale, k/ε, s
ω	=	$\varepsilon/c_\mu k$ (ε turbulent dissipation, $J \cdot m^{-3}s^{-1}$), s
$\dot{\omega}_\alpha$	=	production rate of species α, $kg \cdot m^{-3} \cdot s^{-1}$

I. Introduction

IN hypersonic regime, the laminar-turbulent transition takes place at elevated altitudes, where the flows are in chemical nonequilibrium. The flow is drastically modified both in the boundary layer and wake. This transition corresponds in some cases to the maximum heat-flux trajectory point and is then a driver for assessment of thermal protection. The chemical nonequilibrium is taken into account via the description of chemical species and their kinetics, using a multispecies calculation. This approach is generally made with standard turbulence models (using Reynolds average) giving informations on the averaged quantities $\tilde{T}$, $\tilde{C}_i$, etc. These chemistry-turbulence interactions can be difficult to describe because of the highly nonlinear dependence of the chemical source terms on scalar quantities, such as temperature and composition. Then, the nonlinearity (exponential dependance with T) makes the calculation with averaged values a crude assumption in some cases: $\bar{\dot{\omega}}$ can be significantly different from $\dot{\omega}(\tilde{T}, \tilde{C}_\alpha)$ when the temperature is low compared with the activation temperature of the reaction. This effect can be anticipated in the wake of the reentry vehicle because of low temperatures, associated with low pressures favorable to nonequilibrium.

The emphasis of this Note is on the modeling of turbulent reactive flows to predict the flows around the hypersonic space probe. Two-equation turbulence models have been used for many years, becoming an important tool for engineers in industry. These models produce fairly accurate results for a wide range of applications, and they are computationally rather cheap. Also, we will use one of these models for the turbulence modeling. To model the chemistry-turbulence interactions, Narayan and Girimaji,[1] using the moment method, have proposed a model for turbulent reacting flow. Recently, Baurle et al.,[2] based on this work, have developed an accurate method to model the very high-speed compressible flows. Because of the strong compressibility of the problem, this method seems the best adapted.

This taking into account of the chemistry-turbulence interactions will considerably modify the flow and species fields in the near wake.

II. Mathematical Modeling

A. Governing Equations

Let us consider the Favre-averaged conservative balance equations for mass fraction for ne chemical species, momentum, and total energy. If a chemical reaction can be expressed in the general form

$$\sum_{\alpha=1}^{ne} \nu_\alpha'^{(k)} A_\alpha \rightleftharpoons \sum_{\alpha=1}^{ne} \nu_\alpha''^{(k)} A_\alpha$$

where $\nu'^{(k)}$ and $\nu''^{(k)}$, respectively, are stochiometric coefficients in the forward and backward directions, A_α is a chemistry specie of considered gas, then the production rate of specie α will be evaluated based on the law of mass action:

$$\dot{\omega}_\alpha = \mathcal{M}_\alpha \sum_{k=1}^{n_r} \left[\nu_\alpha''^{(k)} - \nu_\alpha'^{(k)}\right] \left[K_f^{(k)} \prod_{s=1}^{ne} \left(\frac{\rho_s}{\mathcal{M}_s}\right)^{\nu_s'^{(k)}} - K_b^{(k)} \prod_{s=1}^{ne} \left(\frac{\rho_s}{\mathcal{M}_s}\right)^{\nu_s''^{(k)}} \right] \quad (1)$$

with K_f and K_b, respectively, the reaction-rate coefficients in forward and backward directions described by the Arrhenius law:

$$K_{f,b} = AT^n \exp(-T_A/T)$$

We can now express the used turbulence models to close these equations.

Presented as Paper 2004-2339 at the AIAA 34th Fluid Dynamics Conference, Portland, OR, 28 June–1 July 2004; received 24 January 2005; revision received 11 April 2005; accepted for publication 15 August 2005.

*Research Scientist, B.P. 2, Department of Studies and Validation/Service Informatique Scientifique, Centre d'Étude Scientifique et Technique Aquitaine; ngoc-thanh-ha.nguyen-bui@cea.fr.

†Director of Research, B.P. 2, Direction, Centre d'Étude Scientifique et Technique Aquitaine; georges.duffa@cea.fr.

B. Turbulence $k-\omega$ Model (1998)

The performance of the revised $k-\omega$ model[3] is similar to the first in 1988, but the modification of turbulent coefficients makes it possible to improve the undesirable freestream dependency [Eqs. (2) and (3)]. To predict better the laminar-turbulent transition, the damping functions for low turbulent Reynolds number Re_t must be used:

$$\frac{\partial \bar{\rho} k}{\partial t} + \frac{\partial \bar{\rho} \tilde{U}_j k}{\partial x_j} = \frac{\partial}{\partial x_l}\left[\left(\mu + \sigma^* \mu_t\right)\frac{\partial k}{\partial x_l}\right] - \bar{\rho}\widetilde{u_i u_j}\frac{\partial \tilde{U}_i}{\partial x_j} - \beta^* \rho \omega k \tag{2}$$

$$\frac{\partial \bar{\rho} \omega}{\partial t} + \frac{\partial \bar{\rho} \tilde{U}_j \omega}{\partial x_j} = \frac{\partial}{\partial x_l}\left[(\mu + \sigma \mu_t)\frac{\partial \omega}{\partial x_l}\right] - \alpha \frac{\omega}{k}\bar{\rho}\widetilde{u_i u_j}\frac{\partial \tilde{U}_i}{\partial x_j} - \beta \rho \omega^2 \tag{3}$$

with

$$\mu_t = \alpha^* \bar{\rho}\frac{k}{\omega}$$

$$\alpha^* = \frac{\alpha_0^* + Re_t/R_k}{1 + Re_t/R_k}, \qquad \alpha = \frac{13}{25}\frac{\alpha_0 + Re_t/R_\omega}{1 + Re_t/R_\omega}(\alpha^*)^{-1}$$

$$\alpha_0^* = \frac{1}{3}\beta_0, \qquad \alpha_0 = \frac{1}{9},$$

$$\beta = \beta_0 f_\beta, \qquad \beta_0 = \frac{9}{125}$$

$$f_\beta = \frac{1 + 70\chi_\omega}{1 + 80\chi_\omega}, \qquad \chi_\omega = \left|\frac{\Omega_{ij}\Omega_{jk}S_{kl}}{\left(\beta_0^* \omega\right)^3}\right|$$

$$\beta^* = \beta_0^* \frac{4/15 + (Re_t/R_\beta)^4}{1 + (Re_t/R_\beta)^4} f_{\beta^*}, \qquad \beta_0^* = \frac{9}{100}$$

$$f_{\beta *} = \frac{1 + 680\chi_k^2}{1 + 400\chi_k^2}, \qquad \chi_k = \frac{1}{\omega^3}\frac{\partial k}{\partial x_j}\frac{\partial \omega}{\partial x_j}$$

$$\sigma = 0.5, \qquad \sigma^* = 0.5, \qquad R_\beta = 8$$

$$R_k = 6, \qquad R_\omega = 2.95$$

The tensors Ω_{ij} and S_{ij} are the mean rotation and mean strain-rate tensors.

Here χ_ω, equal to zero for two-dimensional plane flows, is a correction for axisymmetric flows; and χ_k, similar to the cross diffusion of Menter model,[4] is added to reduce the freestream dependency of the $k-\omega$ model. The pressure work term $-\overline{u_i''}(\partial \bar{P}/\partial x_i)$ is proportional to density/velocity correlation. It is modeled by the approximation

$$-\overline{u_i''}\frac{\partial \bar{P}}{\partial x_i} = \frac{\mu_t}{\sigma_\rho}\frac{\partial \bar{\rho}}{\partial x_i}\frac{\partial \bar{P}}{\partial x_i} \tag{4}$$

C. Turbulence-Chemistry Closure Model

To calculate a hypersonic flow, a classical turbulent combustion model has not been used because of a very large range of the pressure in the flow. The characteristic convection time is of the same order of magnitude as the characteristic chemical one. We thus cannot consider the approach of very fast chemistry. Also the Narajan and Girimaji[1] model makes it possible to bring to closure directly the production rate $\overline{\dot{\omega}_\alpha}$:

$$\overline{\dot{\omega}_\alpha(T, \rho_\alpha)} = \int_{-0}^{+\infty}\int_0^1 \cdots \int_0^1 \dot{\omega}_\alpha \tilde{\mathcal{P}}(\hat{T}, \hat{\rho}_1, \ldots, \hat{\rho}_\alpha, \ldots, \hat{\rho}_{\text{ne}}) \times \mathrm{d}\hat{T}\,\mathrm{d}\hat{\rho}_1 \ldots \mathrm{d}\hat{\rho}_\alpha \ldots \mathrm{d}\hat{\rho}_{\text{ne}} \tag{5}$$

$\tilde{\mathcal{P}}$, the joint probability density function (PDF) of temperature T and composition ρ_α, has been written as follows:

$$\tilde{\mathcal{P}}(\hat{T}, \hat{\rho}_1, \ldots, \hat{\rho}_\alpha, \ldots, \hat{\rho}_{\text{ne}}) = \tilde{\mathcal{P}}(\hat{T})\tilde{\mathcal{P}}(\hat{C}_1, \ldots, \hat{C}_\alpha, \ldots, \hat{C}_{\text{ne}})\delta(\rho - \bar{\rho}) \tag{6}$$

which assumes statistical independence between the temperature, composition, and density.

Using this definition of the joint PDF $\tilde{\mathcal{P}}$, we can write the production rate $\overline{\dot{\omega}_\alpha}$ into the form[2]

$$\overline{\dot{\omega}_\alpha(T, \rho_\alpha)} \approx \sum_{k=1}^{n_r}[\overline{K_f(T)} \cdot \overline{f_{\rho,f}} - \overline{K_b(T)} \cdot \overline{f_{\rho,b}}]^{(k)} + C_l \sum_{k=1}^{n_r}\left[\left(\overline{K_f'^2} \cdot \overline{f_{\rho,f}'^2}\right)^{\frac{1}{2}} - \left(\overline{K_b'^2} \cdot \overline{f_{\rho,b}'^2}\right)^{\frac{1}{2}}\right]^{(k)} \tag{7}$$

C_l denotes the cross-correlation coefficient between the temperature and composition fluctuations. This method consists of linearizing the variation of the species concentration in function of the temperature [$C_\alpha = \tilde{C}_\alpha + R_m(T - \tilde{T})$]. The quantity R_m can be evaluated like the rate between the reaction source of the species equation and the one of the temperature equation. Also the instantaneous species can be only expressed in function of the temperature; this makes possible the evaluation of C_l depending only on temperature.

Because the computation time is very important for this studied case and it is too important to estimate this coefficient, in this work we take $C_l = 0$. That signifies the used model assumes the statistical independence between temperature and composition. This omission is a serious defect, but this approach has provided some plausible results.[1,5] However, C_l will be taken into account in the further work.

The assumed PDF of temperature is expressed by a Gaussian function $\tilde{\mathcal{P}}(\hat{T}, \widetilde{T''T''})$ and the assumed PDF of composition by a multibeta PDF $\tilde{\mathcal{P}}(\hat{C}_1, \ldots, \hat{C}_\alpha, \ldots, \hat{C}_{\text{ne}}, \sigma_C)$.

Two transport equations of variance are added:

$$\frac{\partial \bar{\rho}\widetilde{h''^2}}{\partial t} + \frac{\partial \bar{\rho}\tilde{U}_j\widetilde{h''^2}}{\partial x_j} = \frac{\partial}{\partial x_l}\left[\left(\frac{\lambda}{C_p} + \frac{\mu_t}{Pr_t}\right)\frac{\partial \widetilde{h''^2}}{\partial x_l}\right] + 2\frac{\mu_t}{Pr_t}\frac{\partial \tilde{h}}{\partial x_j}\frac{\partial \tilde{h}}{\partial x_j} - C_h\frac{\bar{\rho}\widetilde{h''h''}}{\tau} \tag{8}$$

$$\frac{\partial \bar{\rho}\sigma_C}{\partial t} + \frac{\partial \bar{\rho}\tilde{U}_j\sigma_C}{\partial x_j} = \frac{\partial}{\partial x_l}\left[\bar{\rho}(\mathcal{D} + \mathcal{D}_t)\frac{\partial \sigma_C}{\partial x_l}\right] + 2\bar{\rho}\mathcal{D}_t\sum_{\alpha=1}^{\text{ne}}\frac{\partial \tilde{C}_\alpha}{\partial x_j}\frac{\partial \tilde{C}_\alpha}{\partial x_j} - C_{\sigma C}\frac{\bar{\rho}\sigma_C}{\tau} + 2\sum_{\alpha=1}^{\text{ne}}\overline{\dot{\omega}_\alpha C_\alpha''} \tag{9}$$

where τ is the turbulent integral timescale.

The temperature variance is then recovered from the enthalpy variance by neglecting the turbulent fluctuations on the specific heat:

$$\widetilde{h''^2} = C_p(\tilde{T}, \tilde{C}_\alpha)\widetilde{T''T''} \tag{10}$$

III. Numerical Results

A. Numerical Methods

The THOT2D software, a thermo-fluid-dynamical code of CEA/CESTA, was built for transonic, supersonic, or hypersonic problems. This code solves the Euler or Navier–Stokes equations in laminar or turbulent regime (two-equation models) for a perfect gas or a multispecies reactive gas for two-dimensional or axisymmetric geometries. It is based on an extension of Roe's approximate Riemann solver[6] applied to reactive flows.[7] The Harten–Yee total-variation-diminishing scheme[8] is used to solve the hyperbolic part of Navier–Stokes equations. The second order of spatial accuracy is obtained using minmod or superbee limiter. This code is validated on many aerodynamic applications in turbulent regime.[5,9]

The validation of THOT2D then is not the aim of this Note and is not developed here.

B. Test Case

The geometrical configuration is a reference axisymmetric reentry capsule defined by ESA/Centre National d'Etudes Spatiales,[10] in the Aurora program. The freestream values correspond to the maximum steady-state heat flux on a Netlander reentry[11]: geopotential altitude of 31 km, velocity 5321 $\mathrm{m \cdot s^{-1}}$, $p_\infty = 19.6$ Pa, and $T_\infty = 141$ K (Mach number of 27.5553). The Mars atmosphere contains 97% of carbon dioxyde (CO_2) and 3% nitrogen (N_2). The wall

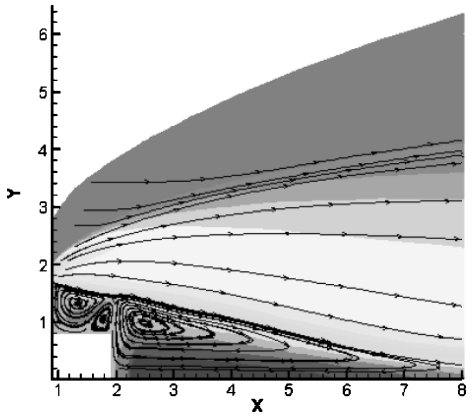

a) Dieudonné et al.[13]

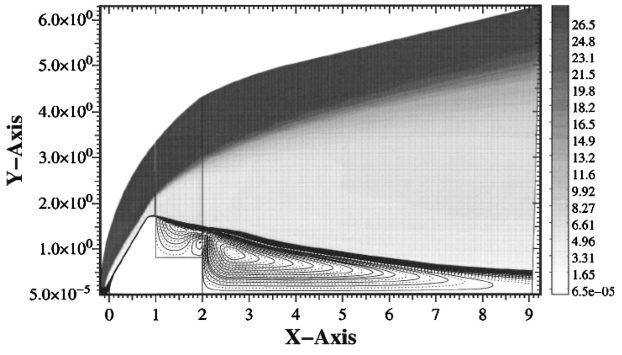

b) This work

Fig. 1 Isomachs, streamlines, and vortex in the near wake.

is noncatalytic, and its temperature is equal to 1500 K at the front of the probe and to 500 K at the back.

Chemical reactions and their kinetics are given by Park et al.,[12] with eight chemical species (CO_2, CO, N_2, O_2, NO, C, N, O) and 12 reactions.

1. Discussion on Laminar Flow Simulation

The different works presented in the International Workshop on Radiation of High Temperature Gas in Planetary Atmosphere Entry[10] have shown that the flow topology in the base is strongly dependent on the grid. Following the grid used, the size of vortex is very different. For some, the wake closure point is located between 6 to 7 m. However, using an adapted multigrid domain, Dieudonné et al.[13] have been able to observe that the shear is pushed away, and the appearance of the third vortex is a secondary vortex at the tip of the satellite rear corner. The wake closure point is found to be 9 m. Figure 1a shows their results obtained with this mesh. After them, this mesh was especially refined to capture better the shear layer. Dieudonné and coworkers[13] have equally shown that this distance of the reattachment point is strongly dependent on the size of this third vortex.

The first computation of this paper is realized in laminar regime in order to understand better the software behavior of this particular case. We can observe the result obtained by our software THOT2D (Fig. 1b) is similar to the one of Dieudonné.[13] The third vortex is well captured, and the wake closure point is located at 9 m. Also, we can realize the second step, which consists of calculating the flow in turbulent regime, the result of laminar flow simulation enables us to be assured of the quality of the numerical computation in turbulent regime.

2. Turbulent Flow Simulation

The freestream value of k_∞ is fixed at 0.0001% of U_∞^2. Despite this very weak imposed intensity, the turbulence even is released. In effect, on Fig. 2 the wall heat flux shows a laminar-turbulent transition zone at the front shield. This increase of the heat flux be-

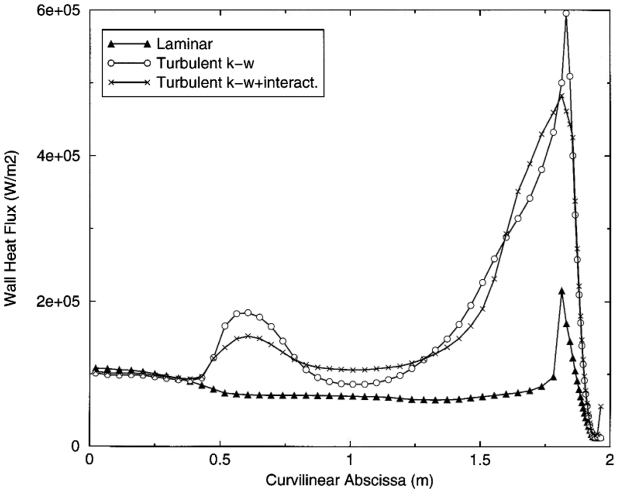

Fig. 2 Forebody wall heat flux.

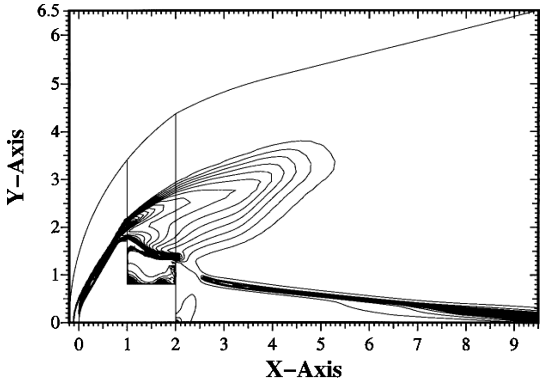

Fig. 3 Turbulent intensity $\sqrt{k}/U$.

comes important by getting farther away from the stagnation point. This confirms an increase of turbulent intensity in the recompression zone. The calculation with chemistry-turbulence interactions gives to us a heat-flux variation less significant than the one without interactions.

In the afterbody flow, the numerical results with fully chemistry-turbulence interactions modeling approximately are the same as the ones obtained by the calculation without interactions. Also we will present only the results with interactions.

The turbulent intensity strongly decreases at the relaxation zone. The double relaxation at the back leads to a relaminarization in the afterbody flow (Fig. 3). Figure 3 plots only the turbulent intensity isolines whose values are inferior to 10%. (For clarity's sake, we omitted the contour labels.) The value of exterior isoline is 0.5%, and then it increases to 10%. The turbulent intensity at the front shield is very important (287%), but it rapidly decreases after the first relaxation at the high corner. This intensity begins to develop in the shear layer and in the first primar vortex, before it decreases at the second relaxation zone. Then, the further shear layer of the base favors the turbulent development in the far wake.

As with the turbulent kinetic energy, the variances $\sqrt{(T''T'')}/T$, σ_C, important at the forebody, decrease after the first relaxation at the high corner. They stay very weak in the base, a suspicion of resumption for enthalpy (or temperature variance) appears.

However, this simulation in turbulent regime shows us that the launching of turbulence at the front shield and a weak turbulent intensity are sufficient for a significant modification of the nearwake at the base. The afterbody temperature is less important in turbulent than in laminar (Fig. 4). Figure 5 plots the axial distribution of temperature in the base; a difference of 500 K is observed between the laminar simulation and the turbulent one. A difference of wall heat fluxes at the rear corner therefore is noticed (Fig. 6). Figure 4 represents the isotherms of both simulations.

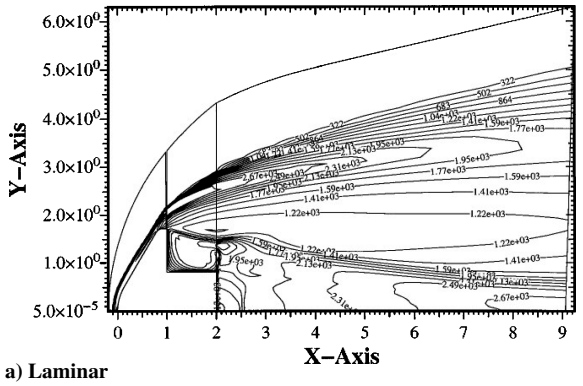

a) Laminar

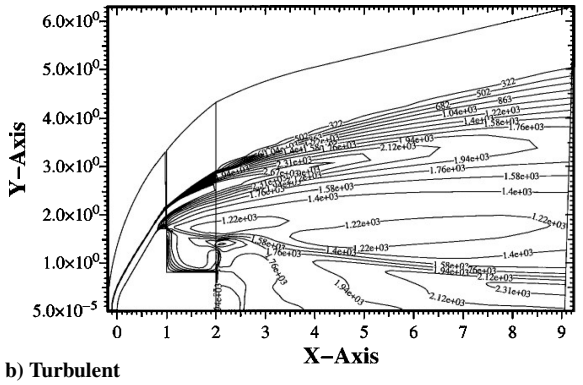

b) Turbulent

Fig. 4 Isotherms.

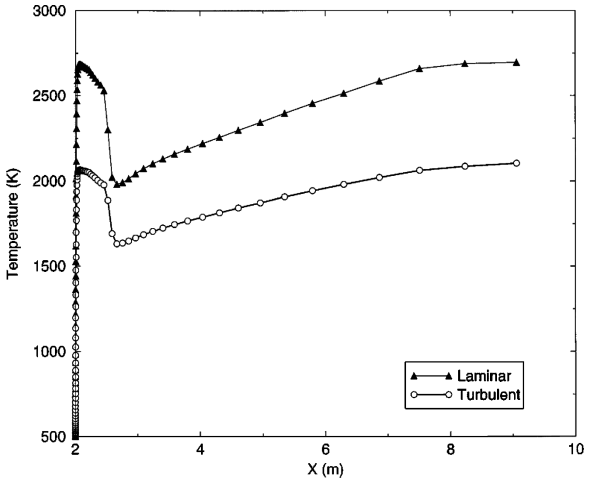

Fig. 5 Axial distribution of temperature.

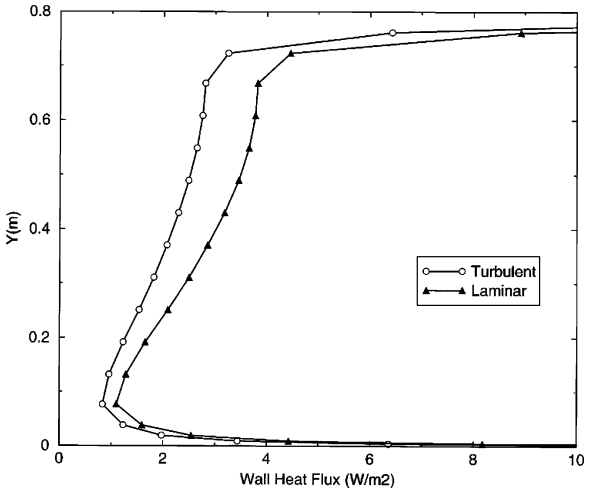

Fig. 6 Wall heat flux in the base.

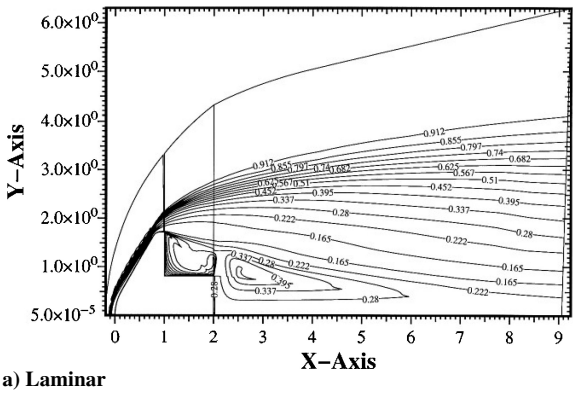

a) Laminar

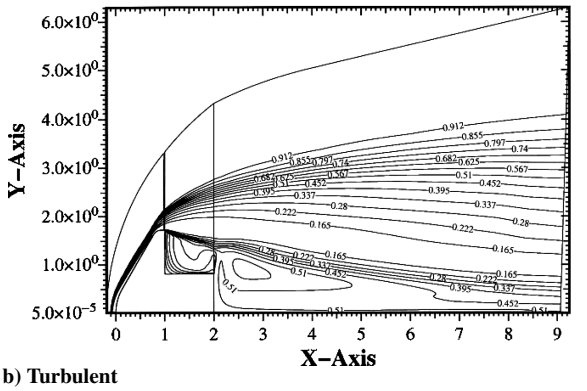

b) Turbulent

Fig. 7 Mass fraction of CO_2.

This temperature field leads to fields of concentration species, which are different than the ones obtained by laminar calculation (Fig. 7). This signifies that the concentration fields of other species are too considerably modified.

IV. Conclusions

The turbulent flow around a hypersonic probe has been performed. This work, even qualitative, stays very interesting because this computation enables us to know how the turbulence modifies the boundary, the flowfields in recirculation zones.

A launching of the turbulence can be observed at the front shield. But the double relaxation zone completely decreases the turbulence intensity. A nonnegligible difference between the temperature fields of laminar and turbulent flows is noticed, thus, the fields of concentration of chemical species. This signifies that even the weak turbulent intensity cannot be ignored in this particular case. This study has shown that the weak turbulence intensity can lead a difference of 500 K on the temperature in the base. This difference is expressed by an augmentation more than 50% of CO_2 in the same zone.

This flow is very sensible to each numerical parameter and to the physical modeling. Very accurate numerical methods and an outstanding physical modeling are necessary to predict this flow. Also, in the further work we will take into account the most possibly accurate all of the turbulent closure approximations.

Because a very strong dependency of the flow morphology of all of the physical-numerical parameters of the computation (grid, numerical methods, physical modeling, . . .), experimentation processes seem to be indispensable to us. Today, only the experimentation makes it possible to understand this flow morphology and to validate the turbulent modeling.

However, the wind-tunnel tests are very difficult to realize in hypersonic regime because at elevated Reynolds numbers they are not reproducible in hot wind tunnels. The tests in flight can provide us with some interesting measurements, for example, the measurements of wall fluxes, or the ones by optical techniques. The wall data have an interpretation limited for turbulence problems, but the optique treatment is able to give the variation in time of some physical variables, which should be used to obtain averaged magnitudes for steady flows.

We can equally notice that an accurate numerical prediction of turbulent reacting flows in hypersonic regime can be applied to optical signature and electromagnetic problems linked to electron and species concentration fluctuations.

References

[1]Narayan, J. R., and Girimaji, S. S., "Turbulent Reacting Flow Computations Including Turbulent Chemistry Interactions," AIAA Paper 92-0342, 1992.

[2]Baurle, R. A., and Girimaji, S. S., "Assumed PDF Turbulence-Chemistry Closure with Temperature-Composition Correlations," *Combustion and Flame*, Vol. 134, No. 1/2, 2003, pp. 131–148.

[3]Wilcox, D. C., *Turbulence Modeling for CFD*, DCW Industries, 1998, p. 121.

[4]Menter, F. R., "Two-Equation Eddy-Viscosity Turbulence Models for Engineering Applications," *AIAA Journal*, Vol. 32, No. 5, 1994, pp. 1598–1605.

[5]Laborde, L., Nguyen-Bui, N. T.-H., Duffa, G., and Caltagirone, J. P., "Turbulent Reacting Flows in Hypersonic Aerodynamics," *Proceedings of 16th International Conference on Numerical Methods in Fluid Dynamics*, Vol. 515, Lecture Notes in Physics, Springer, 1998.

[6]Roe, P. L., "Approximate Riemann Solvers, Parameter Vectors and Difference Schemes," *Journal of Computational Physics*, Vol. 43, No. 2, 1981, pp. 357–372.

[7]Dubroca, B., and Morreeuw, J. P., "An Extension of Roe's Approximate Riemann Solver for the Approximation of Navier–Stokes Equations in Chemical-non-equilibrium Cases," *Proceedings of the 10th Conference on Computing Methods in Applied Sciences and Engineering*, edited by R. Glowinski, Springer-Verlag, 1992.

[8]Harten, A., Warming, R. F., and Yee, H. C., "Implicit Total Variation Diminishing Schemes for Steady States Calculating," AIAA Paper 83-1902, 1983.

[9]Nguyen-Bui, N. T.-H., Dubroca, B., and Ha-Minh, H., "Numerical Prediction of Compressible Turbulent Flows Using $k-\varepsilon$ and Reynolds Stress Closure Model," AIAA Paper 94-2388, 1994.

[10]Charbonnier, J. M., Couzi, J., Dieudonné, W., and Vérant, J. L., "Workshop 2003: Radiation of High Temperature Gas; TC3: Definition of an Axially Symmetric Testcase for High Temperature Radiation Prediction in March Atmosphere Rentry," Centre National d'Etudes Spatiales, NG104-07 TF-001-CNES, Toulouse, France, May 2003.

[11]Charbonnier, J. M., Perraut, P., Dieudonné, W., Spel, M., Carbonne, D., and Couzi, J., "Evaluation of the Aerothermal Heating on the Front Shield of the Netlander Probe During Mars Atmospheric Entry," *Proceedings of AAAF 3rd International Symposium of Atmospheric Reentry Vehicle and Systems*, Arcachon, France, 2003.

[12]Park, C., Howe, J. T., Jaffe, R. L., and Candler, G. V., "Review of Chemical Kinetics Problems of Future NASA Missions. II: Mars Entries," *Journal of Thermophysics and Heat Transfer*, Vol. 8, No. 1, 1994, pp. 9–23.

[13]Dieudonné, W., Spel, M., and Charbonnier, J. M., "Modeling of Sensitivity Analysis for TC3 on Orbiter Aero-Thermal Properties," *Proceedings of the First International Workshop on Radiation of High Temperature Gas in Atmosphere Entry*, edited by B. Warmbein, ESA SP-533, ESA, Noordwijk, The Netherlands, 2003.

R. Kimmel
Associate Editor